Journal of Integrated
SCIENCE & TECHNOLOGY

Deep Learning approach for Co-operative Spectrum Sensing under Congested Cognitive IoT networks

Yogesh Mishra*, Virendra S. Chaudhary

Department of Electronics and Communication Engineering, RKDF University, Bhopal, India.

Received on: 22-Sep-2023, Accepted and Published on: 18-Dec-2023

Article

ABSTRACT

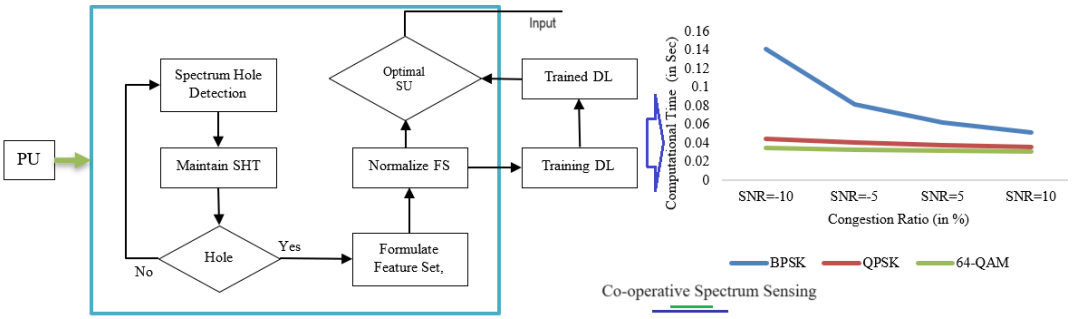

Cognitive radio technology enables intelligent wireless communication systems to learn from their surroundings, allowing secondary users to reuse available radio resources while avoiding interference with licensed users. Spectrum sensing is a critical component, and machine learning approaches are gaining interest for improving performance and predicting spectrum availability. Supporting multiple secondary users simultaneously enhances spectrum sensing speed and data transfer efficiency. The research's second phase introduces a hybrid learning algorithm for Cooperative Spectrum Sensing in congested Cognitive IoT Networks. It evaluates the performance of BPSK, QPSK, and 64-QAM modulation schemes under varying Signal-to-Noise Ratios (SNRs) in a simulated network environment. The hybrid model, incorporating ResNet-50 architecture, adapts to network congestion levels, providing insights for optimizing digital communication systems in diverse congestion scenarios.

Keywords: Cognitive Radio, Spectrum Sensing, Machine Learning, Cooperative Spectrum Sensing, IoT Networks

INTRODUCTION

The ever-growing demand for wireless communication services, along with the increasing proliferation of Internet of Things (IoT) devices, has led to a significant strain on the available radio spectrum resources. Traditional spectrum allocation policies, characterized by static and inflexible frequency assignments, no longer suffice to address this escalating demand. In response to this challenge, the paradigm of Cognitive Radio (CR) has emerged as a transformative solution.[1] Cognitive radio, often regarded as an intelligent and adaptive wireless communication system, has garnered widespread attention for its ability to learn and adapt to its surrounding environment. At its core, CR enables Secondary Users (SUs) to opportunistically access and utilize the radio spectrum allocated to Primary Users (PUs), without causing harmful interference to the licensed users. This paradigm shift from static to dynamic spectrum access holds the promise of significantly improving spectrum utilization, mitigating congestion, and enhancing the overall efficiency of wireless networks.[2] Key to the successful implementation of cognitive radio technology is the process of spectrum sensing, which involves the detection of available spectrum opportunities while avoiding interference with primary users. Spectrum sensing, often carried out in dynamic and challenging wireless environments, presents a critical challenge. Traditional spectrum sensing techniques based on statistical signal processing have shown limitations in coping with the complexity of real-world scenarios, which include variations in signal strength, fading channels, and interference from multiple sources.[3]

In recent years, the fusion of machine learning techniques with spectrum sensing has emerged as a promising avenue to address these challenges effectively. Machine learning, with its ability to learn from data, adapt to changing conditions, and discern complex patterns, offers the potential to significantly enhance the accuracy and robustness of spectrum sensing in cognitive radio networks.[4] This research paper delves into the intersection of Cognitive Radio, Machine Learning, and Spectrum Sensing, with a particular focus

*Corresponding Author: Yogesh Mishra
Email: yogesh.mishra156@gmail.com

Cite as: *J. Integr. Sci. Technol., 2024, 12(4), 778.*
URN:NBN:sciencein.jist.2024.v12.778

on addressing the spectrum congestion challenges faced in the context of IoT networks. The first part of this paper provides an overview of cognitive radio technology and its fundamental principles. It explores the role of spectrum sensing as the cornerstone of CR operation and discusses the limitations of conventional sensing techniques.

The second phase of the research introduces a novel hybrid learning algorithm designed for Cooperative Spectrum Sensing in congested Cognitive IoT Networks. This segment of the study meticulously evaluates the effectiveness and performance metrics of various modulation schemes under varying Signal-to-Noise Ratios (SNRs) in a simulated network environment. The hybrid model, incorporating state-of-the-art machine learning architectures, adaptively learns network congestion levels, thereby providing valuable insights into the optimization of digital communication systems for enhanced efficiency and reliability under diverse network congestion scenarios.[5]

This research investigated the spectrum sensing within 5G networks, a critical process for identifying unused frequency channels and ensuring efficient spectrum allocation. Traditional spectrum sensing methods, while foundational, grapple with limitations such as the need for prior information and time-intensive processes. The introduction of computational intelligence algorithms, particularly deep learning, presents a transformative potential to enhance real-time spectrum sensing capabilities.[6] This research aims to innovate in this domain, developing algorithms that not only predict spectrum availability with greater accuracy but also adapt to the dynamic nature of 5G networks, paving the way for more efficient and robust wireless communication systems.

Therefore, the paper centers on improving spectrum sensing in 5G networks using deep learning algorithms. Traditional methods are inadequate due to their time-consuming nature and the need for prior information about primary users. This research aims to develop advanced computational intelligence algorithms that can efficiently predict channel availability in real-time, enhancing the efficiency of cognitive radio systems. Key objectives include the development of adaptable deep learning algorithms for spectrum prediction, improving the interpretability and reliability of machine learning models, and addressing challenges such as energy efficiency and scalability. This research seeks to overcome the limitations of current spectrum sensing methods, optimizing spectrum utilization in increasingly crowded 5G networks.

Related Work

Patel et al.[1] achieved higher classification accuracy compared to IED and CED using an artificial neural network (ANN). They utilized previous sensing events, Zhang statistics, and energy as input features and optimized hyperparameters. Their ANN outperformed other methods, with a 63% improvement in performance. Pan et al.[2] introduced a deep learning-based method using cyclic spectrum for OFDM signals, improving CNN's performance for spectrum sensing, especially in low SNR scenarios. Soni et al.[3] proposed a deep learning-based LSTM-SS scheme for time series spectrum data, considering PU activity statistics. Their LSTM-SS outperformed ANN-based schemes, even in low SNR conditions. Chen et al.[4] presented a cooperative spectrum sensing system (CSS-CNN) using CNN to enhance detection accuracy in complex scenarios, showing significant improvement. Liu et al.[5] studied hard-biased sensors for off-track reading, considering magnetic noise and the media's magnetic field effects. They proposed a model to calculate reader resistance, particularly important for high-coercivity media. Xu et al.[6] proposed a parallel CNN-LSTM network for single-node spectrum sensing, demonstrating superior performance over a wide range of SNRs and the ability to detect multiple modulation types. Xie et al.[7] developed a deep unsupervised learning-based detector (UDSS) for spectrum sensing, requiring less labeled training data and outperforming non-deep learning algorithms. Sachi et al.[8] presented a comprehensive channel model using CNN for PU signal classification, achieving high accuracy in a noisy environment. Usha et al.[9] analyzed the role of ML algorithms, particularly gradient boosting, for channel state prediction in cognitive radio, achieving high accuracy and energy savings. Liu et al.[10] proposed a big-data-based intelligent spectrum sensing method, processing large spectrum data through ML for heterogeneous spectrum communications. Khan et al.[12] introduced an SVM-based algorithm to classify Secondary Users (SUs) and legitimate Mobile Users (MUs) and used DS evidence theory for decision-making regarding Primary Users' (PUs) existence in the network.

Song et al.[13] explored AI-enabled IoT networks, both centralized and distributed. They focused on technical challenges like random access and spectrum sharing and proposed Deep Reinforcement Learning (DRL) strategies using neural networks for spectrum access and sensing. Delvecchio et al.[14] combined machine learning and communication security to study adversarial evasion attacks. Their approach allows secure communication by evading detection by deep learning-based eavesdroppers. Sagduyu et al.[15] investigated adversarial attacks in IoT networks, focusing on how these attacks affect wireless communication through manipulation of training data. They developed defense mechanisms to counteract these attacks and improve system performance. Lin et al.[16] presented an evaluation framework for UAV sharing using the M/G/1 queuing model. They combined DRL and LSTM networks to improve algorithm performance, demonstrating faster convergence and higher throughput compared to traditional methods. Shi et al.[17] addressed complex signal classification challenges in wireless networks. They used continual learning, outlier detection, extended CNN architectures, and blind source separation for efficient spectrum sharing and signal classification. Zhang et al.[18] introduced a new power control strategy for Secondary Users (SUs) using the A3C methodology and DPPO-based power control. This approach allowed SUs to learn power control strategies independently, enhancing spectrum sharing efficiency. Raj et al.[19] evaluated machine learning techniques for ASD screening using publicly available datasets. Their CNN-based models showed high accuracy in screening across various age groups. Dai et al.[20] focused on annotating retinal lesions in a large image dataset. They applied transfer learning to improve the effectiveness of their Diabetic Retinopathy grading system, achieving high sensitivity and accuracy.

METHODOLOGY USED

System Model

The section discusses a solution for spectrum sharing (SS) and resource allocation in a 5G-based Internet of Things (IoT) network. The designed system, called Hybrid Congestion Aware Cognitive IoT (HCAC-IoT), employs a cluster-based, cognitive radio-assisted architecture specifically designed for urban environments. The network comprises four main components:

- PBS (Primary Base Station)
- HLSAs (High-Level Spectrum Allocators)
- PUs (Primary Users)
- SU (Secondary User)

Entire working is considered to be mobile i.e., PU and SU are mobile. In this network, multiple HLSAs operate under a single PBS within a specified radius. Each HLSA cluster contains a certain number of SUs, which are distributed uniformly within the PBS's coverage area. There is also a variable number of SU in the network with velocity (βSU) and direction of travel (αSU). The mobility of these SU users is defined by two Gaussian-distributed parameters:

$$\beta_{SU}^{v} = N\beta_{\mu}^{v}\mu\beta_{\sigma}^{v} \tag{1}$$

$$\sigma_{SU}^{v} = N\left(\alpha_{\mu}^{v}, 2\pi - \alpha_{\mu}^{v}\tan\left(\frac{\sqrt{\beta_{SU}^{v}}}{2}\right)\Delta t\right) \tag{2}$$

The paper elaborates on the statistical modeling of the mobility of Secondary User (SU) vehicles in the HCAC-IoT system. The mobility is modeled using a Gaussian distribution characterized by mean (μ) and standard deviation (σ).

For each SU vehicle, the mean velocity is denoted by β_{μ}^{v} and its standard deviation is represented by β_{σ}^{v}. Likewise, the mean direction of travel for the SU is denoted by α_{μ}^{v}. The term t specifies the time period during which the mobility model of the SU is updated in the system.

Following this, the section proceeds to describe the roles and responsibilities of each network entity within HCAC-IoT:

PBS: In the HCAC-IoT system, the Primary Base Station (PBS) is a central, stationary unit situated at a fixed location. The PBS serves multiple roles including providing backhaul connectivity to the High-Level Spectrum Allocators (HLSAs). These HLSAs are responsible for managing the SUs located along the urban roads. Additionally, the PBS coordinates spectrum access services across its designated coverage area.

HLSA: In the HCAC-IoT system, the High-Level Spectrum Allocator (HLSA) functions as an intelligent cluster head with various decision-making responsibilities. Primarily, it is tasked with monitoring the Primary User (PU) spectrum occupancy using a Deep Learning-based Spectrum Sharing (DL-based SS) algorithm. Here, ResNet50 is used for spectrum sensing. It maintains a Spectrum Hole Table (SHT) to record available frequencies and manage Secondary User (SU) vehicle requests within its cluster. Secondly, upon receiving a request for opportunistic spectrum access at an SU, the HLSA utilizes a ResNet50 to determine the most optimal SU for channel allocation. The decision-making process for optimal RSU allocation is based on a 3-D feature vector.

Learn Signal Environment: In the HCAC-IoT system model, the first responsibility of the High-Level Spectrum Allocator (HLSA) is to learn the signal environment. This is done through Spectrum Sharing (SS), where the presence or absence of a Primary User (PU) in the network is identified. Based on this identification, a Spectrum Hole Table (SHT) is created. During the SS process, if a PU signal is detected, the corresponding frequency band is marked as "no spectrum hole" (no SH) in the SHT. Conversely, if no PU signal is detected in a particular frequency band, it is labelled as a "spectrum hole" (SH), indicating that these vacant frequency bands of the PU spectrum are available for Secondary Users (SUs) to utilize. The generated SHT serves as a dynamic record of available and occupied spectrum, guiding the HLSA in resource allocation decisions for SU. Thus, the PU detection problem is formulated as expressed in the following:

$$\hat{s}_{PU}^{i} \rightarrow HLSA^{a} = \begin{cases} h^{i} \\ \overline{PU \rightarrow HLSA^{a}\hat{s}_{PU}^{i} + \omega^{i}}, \ (no\ SH) \\ \omega^{i} \quad (SH) \end{cases} \tag{3}$$

Where $\hat{s}_{PU}^{i}$ is the PU signal, $\hat{s}_{PU}^{i} \rightarrow HLSA^{a}$ denotes the ith received PU signal sample at the ath HLSA in the network. $PU \rightarrow HLSA$ denotes the Rayleigh multipath fading channel between the ath HLSA and PBS. ωi denotes the additive white Gaussian noise (AWGN), with σ2 ω noise power and zero mean.

In the technical details of the HCAC-IoT system, $\hat{s}_{PU}^{i}$ represents the signal from the Primary User (PU), and $\hat{s}_{PU}^{i} \rightarrow HLSA^{a}$ denotes the ith received PU signal sample at the ath High-Level Spectrum Allocator (HLSA) in the network. $h_{PU}^{i} \rightarrow HLSA^{a}$ indicates the Rayleigh multipath fading channel between the ath HLSA and the Primary Base Station (PBS). ω^{i} stands for the additive white Gaussian noise (AWGN), which has a noise power of σ_{ω}^{2} and a mean of zero. These elements collectively describe the complexities of the signal environment, accounting for factors like fading and noise, which the HLSA has to consider while making resource allocation decisions based on the Spectrum Hole Table (SHT). This ensures that the system can adaptively manage spectrum sharing and resource allocation in real-world scenarios, where signal quality and availability can be highly variable.

The High-Level Spectrum Allocator (HLSA) calculates the expected stay time of each mobile SU within a target Unit (SU) cell. This is based on the IoT mobility speed and angle of movement. Additional factors like the node density are also considered to identify network conditions. The HLSA also evaluates the network capacity, which is the ratio of resources allocated to active SUs to the total network resources.

Spectrum Sensing using ResNet50

Data Generation: The research involves generating training and validation data in the form of spectrograms, which are visual representations of how the frequency spectrum of a signal changes over time. These spectrograms are categorized into two classes: 1) spectrum hole, representing the absence of Primary User (PU) signal, and 2) no spectrum hole, indicating the presence of PU signal. Each class contains 40,000 spectrograms. The 'spectrum hole' class represents idle PU transmission status, essentially

showing noise, while the 'no spectrum hole' class represents active PU transmission in the network.

Network Architecture: For extraction of features ResNet50 is used, as presented in Fig 1.

ResNet50, with its 50 layers, incorporates residual learning to make training deep networks easier. Like the existing model, ResNet50 also employs Batch Normalization (BN) and Rectified Linear Activation (ReLU) after each convolution, but it leverages the power of shortcut connections to preserve earlier features. These residual connections could further improve multiscale feature learning and model generalization, much like the original model. The residual connections in ResNet50 could also address the issue of vanishing gradient, aiding faster convergence, a feature already present in the existing model. ResNet50 is well-known for its strong performance in a wide variety of applications, potentially improving spectrum sensing accuracy. In last softmax classifier is used for effective resource allocation in the highly dynamic IoV network, as it is currently done by the High-Level Spectrum Allocator (HLSA). By integrating ResNet50, the system might not only retain but potentially enhance its existing capabilities, including efficient spectrum hole detection and resource allocation in HCAC-IoT.

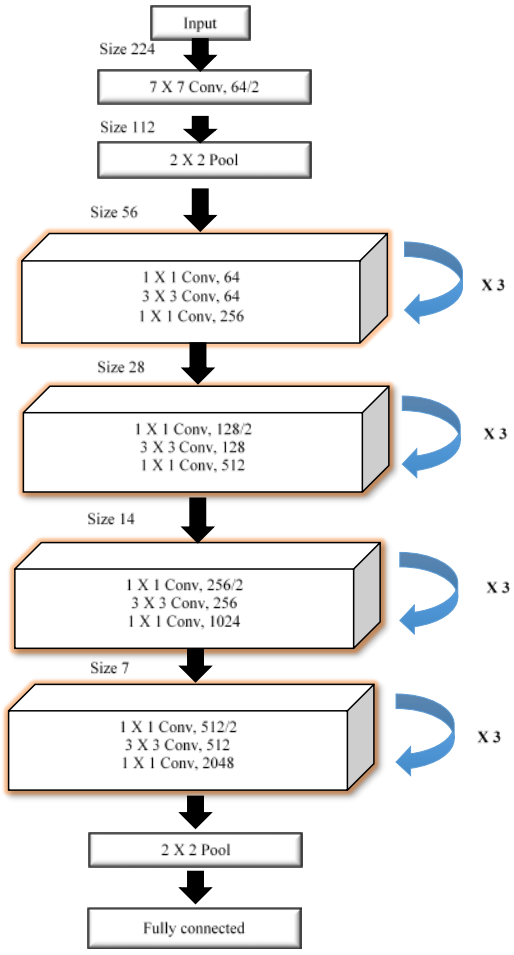

Figure 1. ResNet50 Architecture

Extraction of Learning Features: In the research, different features were initially evaluated to assess the performance. Based on empirical studies, three key features were chosen to optimize spectrum efficiency and resource allocation for SU in the HCAC-IoT system. These features adapt to the changing network conditions, accurately estimating vacant channels and determining optimal network routes for resource allocation. Some of the features are:

Node Density: This feature is defined as the number of active PU and SU within cognitive IoT. Mathematically, the node density in the coverage area of the u_{th}, denoted by v active Secondary User (SU), could be expressed as:

$$f^2 = \delta^u_{RSU} = \sum_{\forall \mu} \mathrm{SU}^v \tag{4}$$

This feature expands the concept of node density to the cluster level, under the jurisdiction of a High-Level Spectrum Allocator (HLSA). For a given a_{th} HLSA cluster that contains u number of SU, the overall node density would incorporate the total number of active Secondary User (SU) node connected to all the SUs within that particular cluster. The node density is evaluated as:

$$\delta^{\alpha}_{HLSA} \sum_{\forall \mu} \delta^u_{RSU} \tag{5}$$

Then it is simplified as:

$$\delta^{\alpha}_{HLSA} \sum_{\forall \mu} \sum_{\forall \mu} \mathrm{SU}^{uv} \text{ active} \tag{6}$$

Network Capacity: This feature defines the network capacity for each u_{th} SU within an a_{th} High-Level Spectrum Allocator (HLSA) cluster. Although the specific formula to express this capacity is not provided, this measure is likely to consider factors such as bandwidth, the number of active users, and perhaps quality of service metrics. Understanding the network capacity of individual RSUs within an HLSA cluster can be crucial for optimizing resource allocation and ensuring a robust and efficient network.

Feature Set: A feature set $FS(v)$ is created by concatenating the computed features sets $\{f_1, f_2, \ldots . f_n\}$ for each SU in a given High-Level Spectrum Allocator (HLSA) cluster. This results in a $(U \times n)$-dimensional feature set, where U is the total number of SUs in the relevant a_{th} HLSA cluster. This feature set is used to train the ResNet50 model with softmax classifier in the HCAC-IoT system. The classifier aims to determine the optimal SU for spectrum access for each Secondary User (SU) node based on the availability of spectrum holes and the best route for resource allocation. Example of feature set is presented as below:

$$FS(v) = \begin{bmatrix} f^1(1,v) & f^2(1,v) & f^3(1,v) \\ f^1(u,v) & f^2(u,v) & f^3(u,v) \\ f^1(U,v) & f^2(U,v) & f^3(U,v) \end{bmatrix} \tag{7}$$

The study uses ResNet50, to dynamically allocate the best SU to handle requests from SU nodes within the HCAC-IoT framework. This approach is shown to be superior to heuristics methods, which are less viable, computationally costly, and sensitive to complex high-dimensional problems. In summary, ResNet50 offers a more

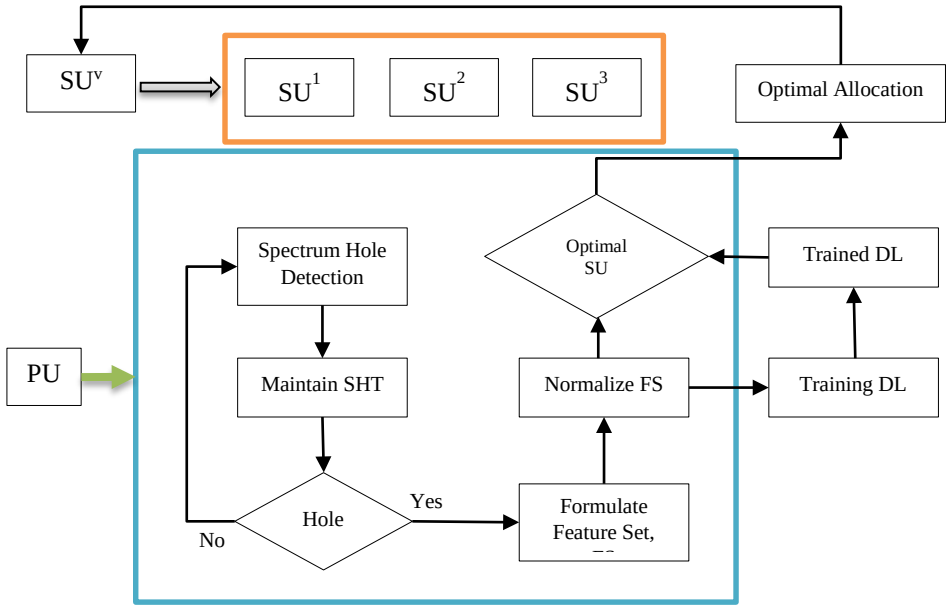

Figure 2. Designed Methodology

efficient and responsive solution for complex, dynamic network environments like HCAC-IoT. The entire working step is presented below in Fig 2.

Result Analysis

The results of the presented work are analyzed on three different metrics under different conditions. These parameters are:
Pd (Probability of Detection): This is a measure of how effectively the system can detect congestion.

RE (Recovery Error Rate): This metric indicates the average error in recovering the true state of the system from the received signals.

Time: This could represent the average computational time taken for each iteration of the algorithm.

Performance Evaluation under a Congested Environment

It seems from Figures 3 to 5 that the system performs best (in terms of detection and recovery error rate) when the network is less congested. It achieves a perfect probability of detection (Pd = 1) when the congestion rate is 0.3 or less. Also, as the congestion rate decreases, the Recovery Error Rate (RE) decreases, suggesting a better recovery performance. The Time metric appears to be relatively consistent across different congestion rates

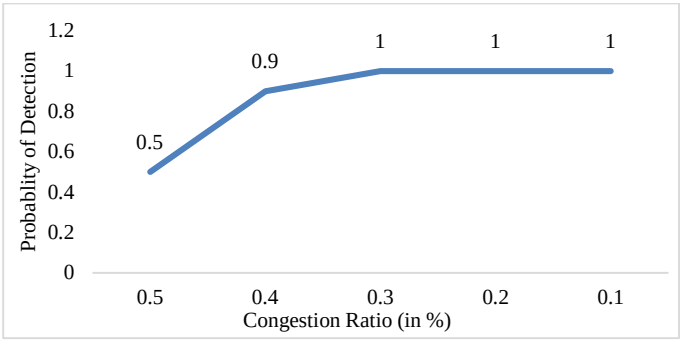

Figure 3. Probability of Detection Under Varying Congestion Ratio

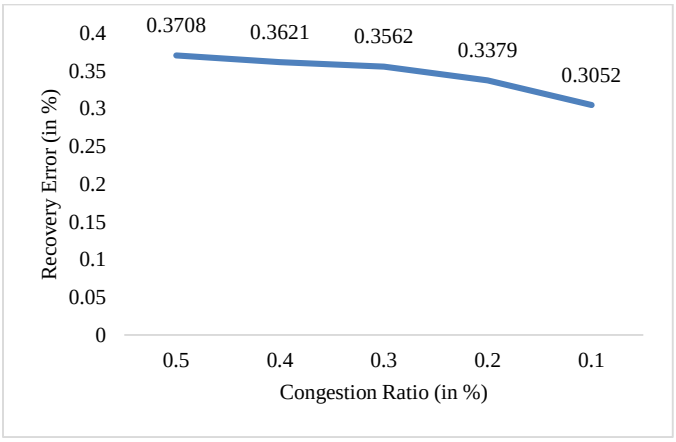

Figure 4. Recovery Error Under Congestion Ratio

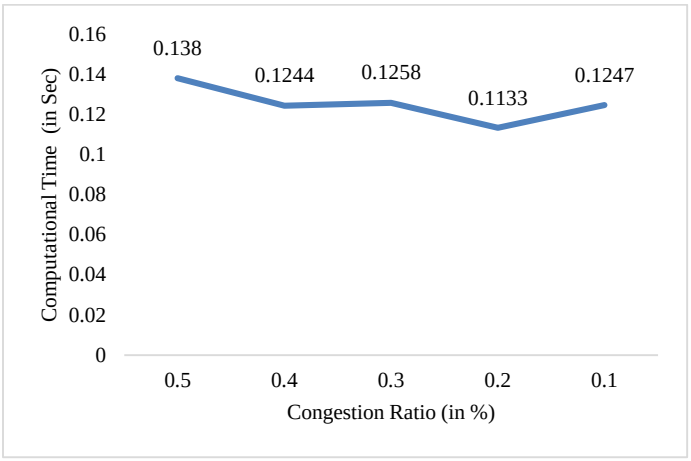

Figure 5. Average Computational Time Under Varying Congestion Ratio

Performance Evaluation under Congested and Noisy Environment

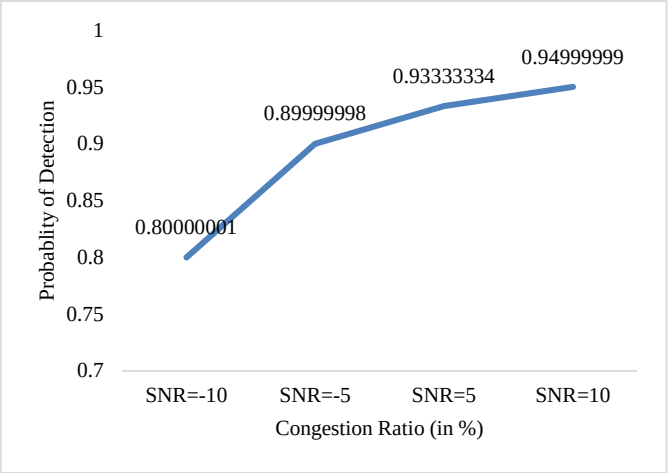

Figure 6. Probability of Detection Under Varying SNR

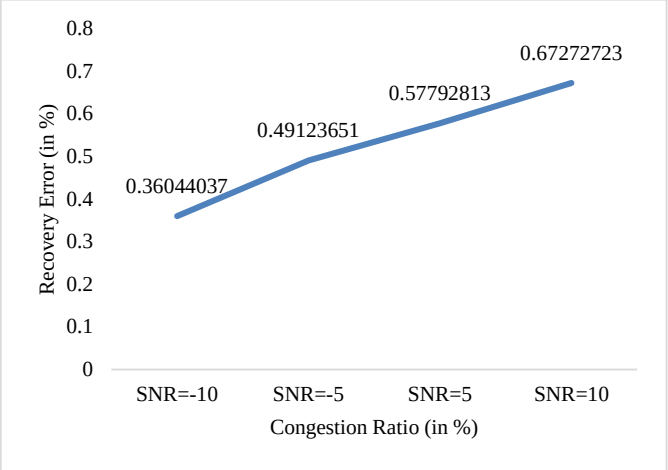

Figure 7. Recovery Error Under Varying SNR

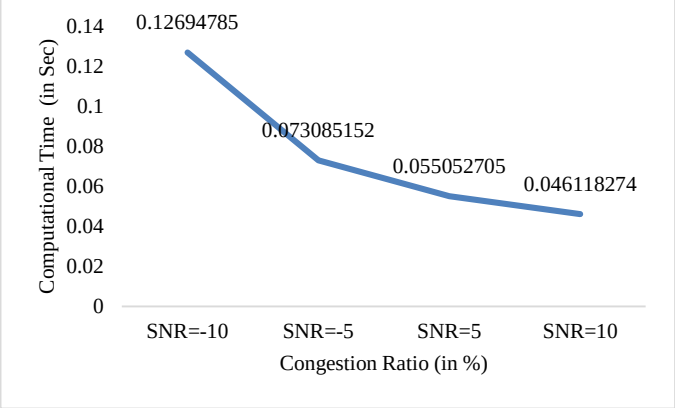

Figure 8. Average Computational Time Under Varying SNR

From figures 6 to 8, the results are presented with varying levels of Signal-to-Noise Ratio (SNR), measured in decibels (dB). Signal-to-Noise Ratio in dB, which represents the power of the signal relative to the power of the background noise. According to the fig 6, as the SNR increases (i.e., less noise or a stronger signal), the Recovery Error Rate also increases, which might be counterintuitive. From fig 7 the PD improves as SNR improves, which is expected. A clearer signal should generally lead to better detection capability. From the fig 8, the computational time decreases as the SNR increases, suggesting that higher-quality signals might require less computational effort to process, or that the algorithm converges faster in such cases. Overall, the figures suggests that higher SNR levels yield better detection capabilities (higher PD) but also lead to higher Recovery Error Rates (higher RE) in this particular simulation. Computational time improves (decreases) as SNR gets better.

Performance Evaluation under Congested and Noisy Environment with BPSK Modulation

Figure 9 presents the Probability of Detection (PD) under different Signal-to-Noise Ratio (SNR) conditions for three different modulation schemes: BPSK (Binary Phase-Shift Keying), QPSK (Quadrature Phase-Shift Keying), and 64-QAM (64-Quadrature Amplitude Modulation). BPSK shows perfect detection (PD = 1) at lower SNRs (-10 dB, -5 dB, 5 dB) but takes a hit at 10 dB (PD = 0.85). The PD of QPSK is generally good but slightly lower than BPSK at negative SNRs. It stays relatively consistent as SNR increases, but like BPSK, also drops slightly at 10 dB. 64-QAM starts with the lowest PD at -10 dB and maintains a slightly lower PD across the board compared to BPSK and QPSK. Its PD also drops at 10 dB, but the drop is similar to that in QPSK. All three modulation schemes perform extremely well in terms of detection capability at lower SNRs but show a noticeable dip in performance at an SNR of 10 dB. BPSK provides the highest Probability of Detection at negative and low positive SNRs, but the differences among the three schemes are not significant. The decline in the Probability of Detection at an SNR of 10 dB across all modulation schemes is an interesting phenomenon that might warrant further investigation. These results provide valuable insights into how different modulation schemes behave under various noise conditions, particularly in terms of their ability to accurately detect true conditions.

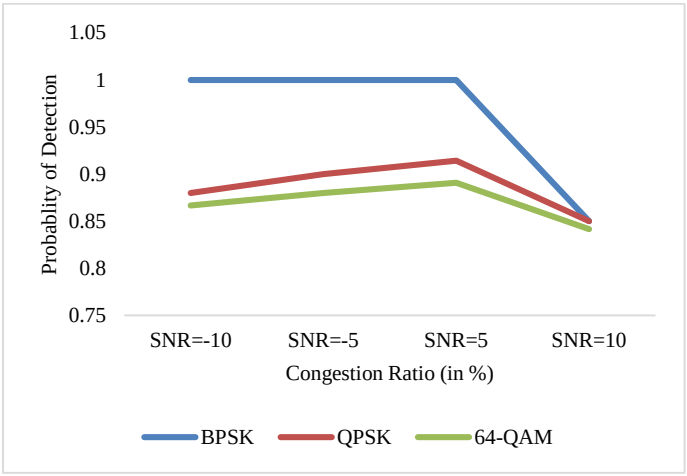

Figure 9. Probability of Detection Comparison with Modulation Techniques

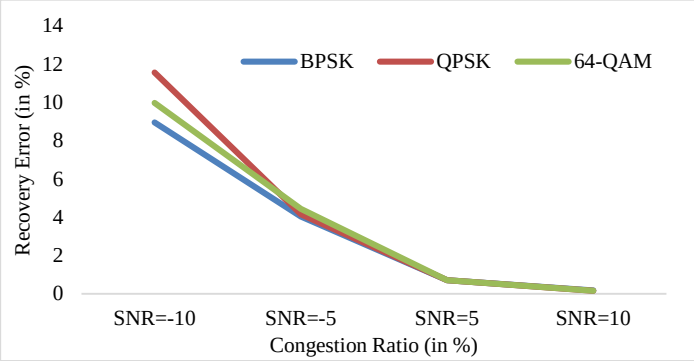

Figure 10. Recovery Error with Modulation Techniques

Figure 10 compares the Recovery Error Rate under varying Signal-to-Noise Ratio (SNR) conditions for three different modulation schemes: BPSK (Binary Phase-Shift Keying), QPSK (Quadrature Phase-Shift Keying), and 64-QAM (64-Quadrature Amplitude Modulation). For all modulation schemes, the Recovery Error Rate is highest at an SNR of -10 dB and decreases substantially as SNR improves. At lower SNRs, BPSK appears to have a slightly lower Recovery Error Rate compared to QPSK. However, this advantage seems to fade away as SNR increases. Interestingly, 64-QAM shows a Recovery Error Rate that is between BPSK and QPSK at -10 dB but is the highest at -5 dB and then aligns closely with the other two at higher SNRs. At an SNR of 10 dB, all three schemes demonstrate a very low Recovery Error Rate, with 64-QAM showing the lowest value. All modulation schemes are sensitive to noise at low SNR levels, but they perform significantly better as the SNR improves. At high SNRs, the Recovery Error Rates across all three modulation schemes are quite similar, suggesting that the choice of modulation may have less impact on recovery performance in high-SNR scenarios. Despite its complexity, 64-QAM performs admirably well, particularly at higher SNRs, even achieving the lowest Recovery Error Rate at an SNR of 10 dB. The varying behavior of these modulation schemes at different SNRs could be a subject for further investigation to understand the intricacies of their performance better. Overall, these results offer useful insights into how well each modulation scheme can recover the true signal under different noise conditions.

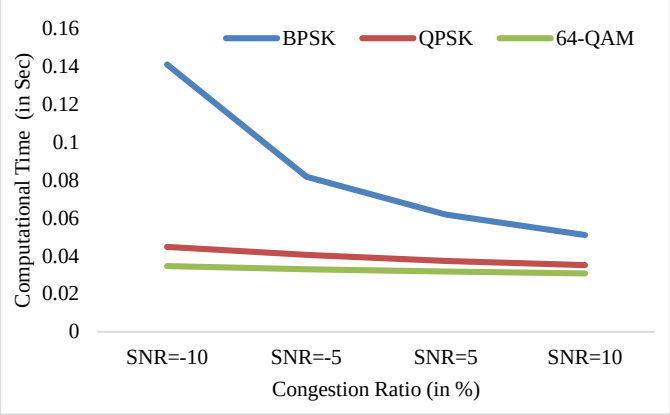

Figure 11. Average Computational Time Comparison with Modulation Techniques

Figure 11 presents the Average Computational Time under different Signal-to-Noise Ratio (SNR) conditions for three modulation schemes: BPSK (Binary Phase-Shift Keying), QPSK (Quadrature Phase-Shift Keying), and 64-QAM (64-quadrature Amplitude Modulation). For BPSK, the computational time is noticeably higher at lower SNRs and decreases as SNR improves. This trend is less apparent for QPSK and 64-QAM. Across all SNR levels, BPSK takes more computational time compared to QPSK and 64-QAM. In general, the average computational time for all schemes seems to decrease as the SNR increases. Despite its complexity, 64-QAM consistently requires the least computational time across all SNR levels. Higher SNRs seem to reduce the computational time required, particularly for BPSK. 64-QAM, despite being the most complex scheme, requires the least computational time, suggesting a high level of efficiency in its implementation. While BPSK has its advantages in other metrics, it falls short in terms of computational efficiency compared to QPSK and 64-QAM. The reduction in computational time with increasing SNR suggests that there might be opportunities for further optimization, especially for schemes like BPSK which start with higher times at lower SNRs.

Conclusion

This study compares the performance of three digital modulation schemes - BPSK, QPSK, and 64-QAM - in a network with different Signal-to-Noise Ratios (SNRs). It finds that all schemes perform adequately at low SNRs, but there's a noticeable performance drop at 10 dB SNR. However, as SNR increases, the Recovery Error Rates decrease, with 64-QAM demonstrating the lowest error rates at higher SNRs. Despite its complexity, 64-QAM proves to be the most computationally efficient, making it an ideal choice for environments with limited resources. Conversely, BPSK, though effective at low SNRs, is computationally inefficient and less suitable for real-time or resource-constrained applications. In summary, 64-QAM offers a good balance of detection capability and computational efficiency, particularly at higher SNRs.

Conflict of Interest

Authors declare that they do not have any conflict of interest for this work.

References

1. D.K. Patel, M. López-Benítez, B. Soni, Á.F. García-Fernández. Artificial neural network design for improved spectrum sensing in cognitive radio. *Wirel. Networks* **2020**, 26 (8), 6155–6174.
2. G. Pan, J. Li, F. Lin. A Cognitive Radio Spectrum Sensing Method for an OFDM Signal Based on Deep Learning and Cycle Spectrum. *Int. J. Digit. Multimed. Broadcast.* **2020**, 2020.
3. B. Soni, D.K. Patel, M. Lopez-Benitez. Long Short-Term Memory Based Spectrum Sensing Scheme for Cognitive Radio Using Primary Activity Statistics. *IEEE Access* **2020**, 8, 97437–97451.
4. Z. Chen, D. Guo, J. Zhang. Deep Learning for Cooperative Spectrum Sensing in Cognitive Radio. *Int. Conf. Commun. Technol. Proceedings, ICCT* **2020**, 2020-October, 741–745.
5. Z. Liu, Z. Yuan, C.L. Ong, S. Ang. Influence of data patterns on reader performance at off-track reading. *IEEE Trans. Magn.* **2014**, 50 (11).
6. M. Xu, Z. Yin, M. Wu, et al. Spectrum Sensing Based on Parallel CNN-LSTM Network. *IEEE Veh. Technol. Conf.* **2020**, 2020-May.
7. J. Xie, J. Fang, C. Liu, L. Yang. Unsupervised Deep Spectrum Sensing: A Variational Auto-Encoder Based Approach. *IEEE Trans. Veh. Technol.* **2020**, 69 (5), 5307–5319.

8. P. Shachi, K.R. Sudhindra, M.N. Suma. Deep Learning for Cooperative Spectrum Sensing. *2020 2nd PhD Colloq. Ethically Driven Innov. Technol. Soc. PhD Ed. 2020* **2020**.
9. N. Usha, K.V. Reddy, N.N. Nagendra. Dynamic spectrum sensing in cognitive radio networks using ML model. *Proc. 3rd Int. Conf. Smart Syst. Inven. Technol. ICSSIT 2020* **2020**, 975–979.
10. X. Liu, Q. Sun, W. Lu, C. Wu, H. Ding. Big-Data-Based Intelligent Spectrum Sensing for Heterogeneous Spectrum Communications in 5G. *IEEE Wirel. Commun.* **2020**, 27 (5), 67–73.
11. C. Gattoua, O. Chakkor, F. Aytouna. An overview of cooperative spectrum sensing based on machine learning techniques. *2020 IEEE 2nd Int. Conf. Electron. Control. Optim. Comput. Sci. ICECOCS 2020* **2020**.
12. M.S. Khan, L. Khan, N. Gul, et al. Support Vector Machine-Based Classification of Malicious Users in Cognitive Radio Networks. *Wirel. Commun. Mob. Comput.* **2020**, 2020.
13. Song, Hao, et al. Artificial intelligence enabled Internet of Things: Network architecture and spectrum access. *IEEE Computational Intelligence Magazine* **2020**, 15(1), 44-51.
14. Delvecchio, Matthew David. Enhancing Communications Aware Evasion Attacks on RFML Spectrum Sensing Systems. Diss. Virginia Tech, **2020**.
15. Sagduyu, Yalin E., Yi Shi, and Tugba Erpek. IoT network security from the perspective of adversarial deep learning. IEEE International Conference on Sensing, Communication, and Networking (SECON). IEEE, **2019**.
16. Lin, Yun, et al. Dynamic spectrum interaction of UAV flight formation communication with priority: A deep reinforcement learning approach. *IEEE Transactions on Cognitive Communications and Networking* **2020**, 6(3), 892-903.
17. Shi, Yi, et al. Deep learning for RF signal classification in unknown and dynamic spectrum environments. IEEE International Symposium on Dynamic Spectrum Access Networks (DySPAN). IEEE, **2019**.
18. Zhang, Haijun, et al. Power control based on deep reinforcement learning for spectrum sharing. *IEEE Transactions on Wireless Communications* **2020**, 19(6), 4209-4219.
19. Raj, Suman, and Sarfaraz Masood. Analysis and detection of autism spectrum disorder using machine learning techniques. *Procedia Computer Science* **2020**, 167, 994-1004.
20. Dai, Ling, et al. A deep learning system for detecting diabetic retinopathy across the disease spectrum. *Nature communications* **2021**, 12(1), 3242.